Deep–Sea Research II xxx (xxxx) xxx

Contents lists available at ScienceDirect

Deep-Sea Research Part II

journal homepage: http://www.elsevier.com/locate/dsr2

Carbon export and drivers in the southeastern Levantine Basin

Ronen Alkalay [a,b,*], Olga Zlatkin [a,b], Timor Katz [b], Barak Herut [b], Ludwik Halicz [c,d], Ilana Berman-Frank [a,e], Yishai Weinstein [a]

[a] Bar-Ilan University, Ramat-Gan, 52900, Israel
[b] Israel Oceanographic & Limnological Research, Haifa, 31080, Israel
[c] Geological Survey of Israel, Jerusalem, 95501, Israel
[d] Biological and Chemical Research Centre, University of Warsaw, 02-089, Warsaw, Poland
[e] University of Haifa, Leon H Charney School of Marine Sciences, Haifa, 3498838, Israel

ARTICLE INFO

Keywords:
C export
^{234}Th
Sediment traps
Levantine basin
DeepLev

ABSTRACT

In this paper, we present C export data from the southeastern Levantine Basin, 50 km west of Haifa, at water depth of 1500 m. Particulate organic carbon (POC) fluxes were measured for 18 months by automated and single bottle sediment traps at the recently-deployed DeepLev observatory and compared with water column profiles of ^{234}Th. Calculations, based on POC/^{234}Th ratios, result in water column-integrated export of 18 mmolC m^{-2} d^{-1} at the end of summer (Dec 2017) and remineralization during spring (e.g. 14.4 mmolC m^{-2} d^{-1}, Apr, 2018). Based on the sediment traps POC export in the basin was generally low (0.05–1 mmolC m^{-2} d^{-1} at the base of the photic zone during Dec 2017–May 2018). Fluxes were quite variable, and the export pattern was mainly controlled by coastal discharge or shelf-resuspension (winter peaks) rather than by marine primary production. This was demonstrated by: i) larger POC fluxes measured by deep water (1300 m) and twilight zone (280 m) traps compared to fluxes measured at the base of euphotic zone, ii) tight correlation of POC with total mass flux, iii) decrease of the POC percentage during winter peak events and iv) imbalance (large integrated deficit or excess) of water column ^{234}Th. Both deficit and excess are evidence of lateral flux, where the first probably results from wave-induced shelf resuspension of organic-poor material, which underwent minimal remineralization and induced scavenging, while the latter derives from the conveyance of large amount of land-derived organic matter, which undergoes remineralization, therefore input of ^{234}Th to the water column.

1. Introduction

About 10–30% of the net primary production, produced in the oceans photic zone, is exported downwards by the biological pump (Falkowski 1998; Boyd and Trull, 2007; Henson et al., 2012; Siegel, 2014). This pump is an important buffering agent of atmospheric CO_2, and it forms significant foundation for most of the heterotrophic life in the deep-sea. It is commonly estimated that only 20% of the export is in the dissolved form (hereafter: DOM), while 80% settles as particulate matter (POM, e.g. Carlson et al., 1994; Hansell et al., 2009), mainly via passive sinking of aggregates and fecal pellets (Armstrong et al., 2009; Wakeham et al., 2009), aided by mineral ballast (e.g. Honjo, 1996; Klaas and Archer, 2002; Armstrong et al., 2002, 2009). Nevertheless, in oligotrophic areas, <10% of the primary production is exported and the POM:DOM flux ratio changes in favor of the dissolved flux. In the eastern Mediterranean Sea (hereafter: EMS), observations and modelling suggest that particulate flux represents just 10% of total export, with the predominant carbon exported as dissolved organic carbon (Guyennon et al., 2015; Ramondenc et al., 2016).

Of the exported carbon, usually only ca. 10% survives the travel through the oceanic Twilight Zone (TLZ, i.e. 200 to ~1000 m depth) and reaches the deep, Dark Zone (e.g. Martin et al., 1987; Buesseler and Boyd, 2009), with a parallel decrease in the POM:DOM ratio (e.g. Thomas et al., 1995; Hansell et al., 2009).

Carbon export in the Mediterranean Sea is relatively low (1–13% of primary production (PP), Moutin and Raimbault, 2002; Ramondenc et al., 2016). It has been mainly studied in the western basin, near the coast of France (Roy-Barman et al., 2002; Speicher et al., 2006; Kessouri et al., 2018) and the Balearic Sea (Danovaro et al., 1999; Gogou et al., 2014). It has been also investigated in the Ionian Sea and the western part of the Levantine Basin (Moutin and Raimbault, 2002; Speicher et al., 2006; Stavrakakis et al., 2013), while there is hardly any data from

* Corresponding author. Bar-Ilan University, Ramat-Gan, 52900, Israel.
E-mail address: ronen.alkalay@gmail.com (R. Alkalay).

https://doi.org/10.1016/j.dsr2.2019.104713
Received 31 January 2019; Received in revised form 13 December 2019; Accepted 15 December 2019
Available online 18 December 2019

the eastern Levantine Basin.

The Levantine Basin is a highly oligotrophic sea, with extremely low nutrient concentrations (e.g. nitrate and phosphate concentrations of «1 and < 0.03 μmol kg^{-1}, respectively Krest et al. 2014 (Kress et al., 2013; Krom et al., 2004; Lazzari et al., 2016; Ozer et al., 2015); and primary production of 60–80 gC m^{-2} yr^{-1} (Azov, 1986; Psarra et al., 2000). Depletion in dissolved inorganic P (DIP) in early spring is the primary limiting nutrient for EMS PP (Krom et al., 1991; Zohary and Robarts, 1998; Van-Wambeke et al., 2002; Tanaka et al., 2009). From spring through summer, DIN (dissolved inorganic nitrogen) limitation or DIN-DIP co-limitation also occurs due to continued N recycling, auto-heterotroph competition and inorganic-organic pool transfer (Thingstad et al., 2005; Tanaka et al., 2011). The Levantine Basin is also a warm sea, with surface water temperature varying between 17-27 °C and deep water typically >13 °C. Its ultra-oligotrophic nature results in a highly transparent and relatively deep photic zone (Berman et al., 1985). Attenuation of surface light to 1% occurs between 75 to 125 m (Berman et al., 1984) and 0.1% of the incident irradiance is recorded at ~180 m. Being relatively close to shore, the deep Levantine Basin could also be subjected to land-derived input, as well as to Sahara-originated dust (Herut et al., 1999, 2002; Gogou et al., 2014), which could both significantly affect fluxes toward the seafloor.

In this study, the first of its kind in this area, we used direct measurements by automated sediment traps (Honjo and Doherty, 1988; Yu et al., 2001) and the $^{234}Th/^{238}U$ disequilibrium method (Buesseler et al., 1992; Benitez-Nelson et al., 2001; Waples et al., 2006) to study patterns and drivers of POC export at the deep southeastern Levantine Basin, ca. 50 km from shore.

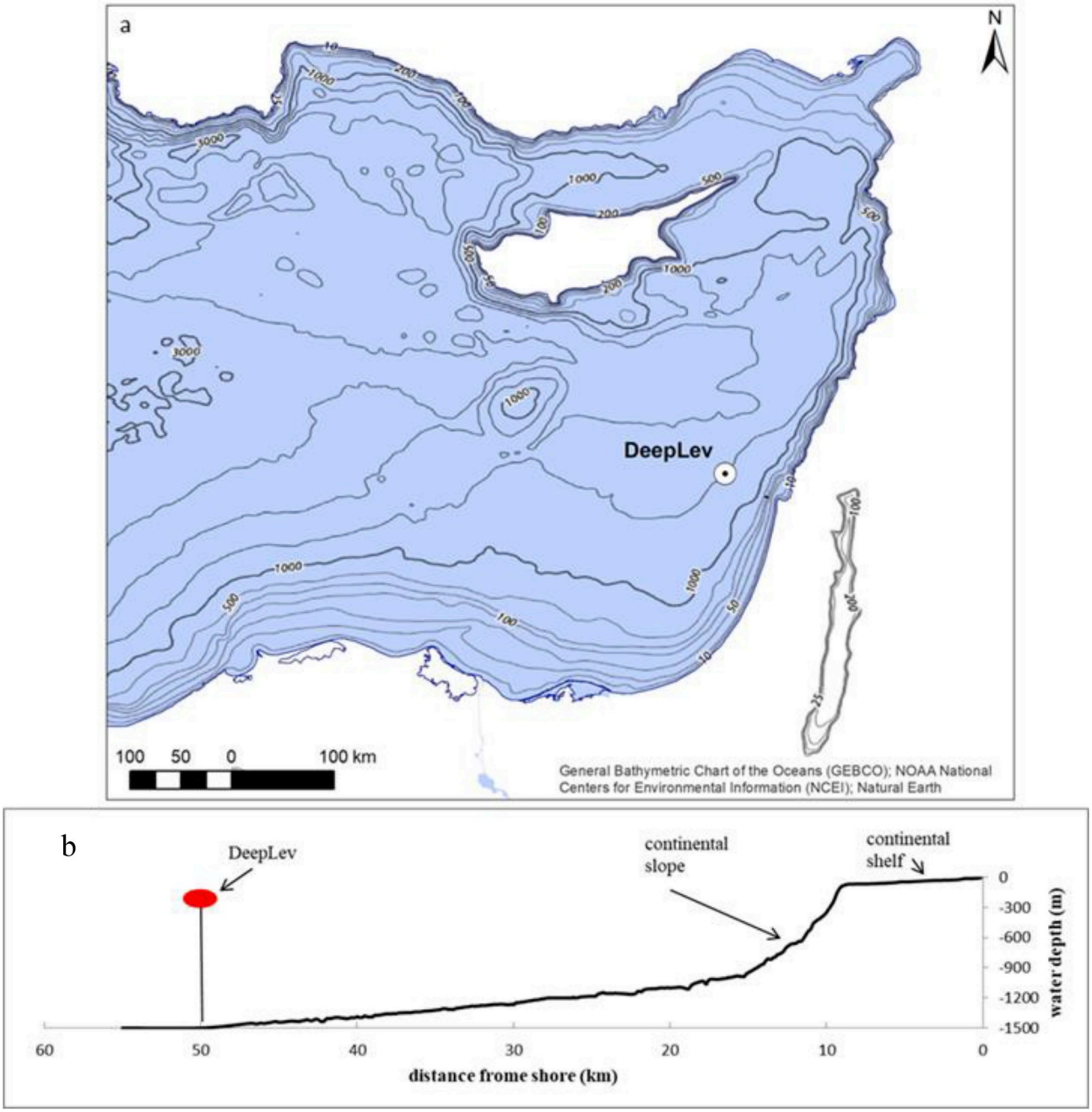

Fig. 1. (a) Location map of the DeepLev mooring; (b) E-W bathymetric profile from shore to the DeepLev location.

2. Methods

2.1. Study site and field work

The DeepLev observatory (Fig. 1) is a bottom-tethered mooring array, located 50 km west of Haifa, at 1500 m depth (Lat/Lon: 32° 59′ 58.2000″ N, 34° 29′ 58.8120″ E). Three McLane automated traps (PARFLUX Mark78H-21) and two single bottle cylindrical sediment traps (Hydro-Bios) were positioned along the cable at depths of 180 (base of the photic zone), 280, 1,300, 810 and 1490 m, respectively. The mooring was deployed for three consecutive periods of ca. 180 days each during Dec 2016–May 2018. A detailed position and system set-up are described by Katz et al. (this issue).

During visits to the DeepLev site onboard the R/V Bat Galim, water column profiles (9–13 depths, down to 1300 m, 200 m above seafloor) were also sampled (2–4 L) for ^{234}Th (and ^{238}U) measurements, using a 12-Niskin bottle rosette.

2.2. Sediment traps

The McLane traps are conical and have an aperture area of 0.5 m^2. Each trap is loaded with a carousel of 21 500-ml bottles, which produce time series of particulate matter fluxes. The bottles were filled with deep seawater containing 4% formaldehyde as a fixative and buffered with borate to pH = 7.3 (modified from Buesseler et al., 2007; no buffering took place during Nov 2016–May 2017). The bottles of the cylindrical traps were alternatively filled with saturated brine solution. After retrieval, the sampling bottles were removed from the traps and were kept refrigerated until processing in the laboratory following the procedure described by Heussner et al. (1990a) and Lamborg et al. (2008).

During the first 6-month deployment (Nov 2016 through May 2017), large schools of fish (*Paralepis coregonoides*, Stern et al., 2019), were captured by the two shallow traps and filled the collection bottles. We tried to address this problem by covering the traps with a fishing net (May-Nov 2017), which did not solve the problem. During the third deployment period (Dec 2017 through May 2018), the McLane sediment trap tops were covered by a 7 mm stainless steel mesh, which mostly prevented access of the fish. Accordingly, the report for the first year includes only the 1300 m trap and the cylindrical traps, while results from the three McLane traps are presented only for Dec 2017–May 2018.

Samples collected in the bottles were treated at the laboratory according to a protocol adapted from Centre de Formation et de Recherche sur l'Environnement Marin (CEFREM, Heussner et al. 1990a). After decantation and removal of large swimming organisms, the samples were wet-split, using a WSD-10 wet sample divider, into ten sub-samples. Two 25 mm GFF filters (nominal pore size 0.7 μm), containing 3% of the total mass each, were measured for ^{234}Th, and another four filters were used for carbon and nitrogen (POC:PN) determination. In the last sampling period (Dec 2017–June 2018), POC was analyzed on freeze-dried material instead of the filters.

2.3. Water column ^{234}Th

Thorium is highly particle-reactive, and as such is a good tracer for particle transport in a water body. ^{234}Th, with half-life of 24.1 d, is commonly used as a tracer for biogeochemical processes, in particular C export, on the time scale similar to particle dynamics in the upper ocean (several weeks, e.g. Waples et al., 2006). Water samples (4 L) were acidified with HNO_3 immediately after sampling and spiked with ^{230}Th (10 dpm), which was used as a yield monitor (Pike et al., 2005). Then, the samples were allowed to equilibrate. After adjusting pH to 8.0–8.2 by adding a NH_4OH buffer solution, $KMnO_4$ (0.375 ml, 3 g/l) and $MnCl_2$ (0.25 ml, 8.0 g/l) solutions were added, followed by an overnight equilibration, in order to allow co-precipitation of thorium with Mn oxides (e.g. Benitez-Nelson et al., 2001; Buesseler et al., 2001; Rutgers van der Loeff et al., 2006). Samples were then vacuum-filtered through 47 mm quartz microfiber (QMA) filters (nominal pore size 1 μm) and dried at 50 °C.

2.4. Analytical methods

2.4.1. ^{234}Th and ^{238}U

Filters (25 mm diameter) of particulate matter from the sediment traps and 19 mm filter punches of MnO_2 precipitates of water column samples were mounted on designated Nylon disks, covered with LDPE film and measured by a RISO Laboratories gas flow beta multi-counter. Samples were recounted after 5–6 months to determine background radioactivity due to beta decay of long-lived natural radionuclides (Buesseler et al., 2001; Pike et al., 2005). The beta counter was calibrated against IRMM ^{238}U standards, which were spiked onto filters covered by MnO_2 precipitates. After final counting, the MnO_2 precipitates were dissolved by HNO_3+HF and thorium was pre-concentrated using an AG1-X8 resin-filled column (Pike et al., 2005). ^{230}Th was then analyzed by a NU Instruments MC-ICPMS in the Geological Survey of Israel, using a^{229}Th spike in order to determine the thorium yield. Calculated thorium yields averaged 98%, with a few samples <90% (down to 73%), which were corrected accordingly.

Rutgers van der Loeff and Moore (1999) and others (e.g. Benitez-Nelson et al., 2001; Cai et al., 2006) adopted a protocol, which includes covering of samples with a thick (or double layer) Al foil, as to stop the weak beta particles of ^{234}Th and mostly measure the stronger betas of its daughter, ^{234}Pa. Since this protocol was not followed in this study, we determined the attenuation factor of beta counting by a double Al foil of both MnO_2 precipitates of seawater samples and of several ^{238}U standards. The first yielded 0.59 ± 0.05 (n = 10) and the latter: 0.*61* ± 0.08 (n = *6*), which is in pretty good agreement. The attenuation factor measured on sediment particles yielded very similar results (0.63 ± 0.11, n = 5).

Uranium was determined by ICP-MS (PerkinElmer, NexION 300D) after 1:20 dilution of seawater with 0.1 N HNO_3. Each measurement was based on 3 runs, and the analysis included repeated determinations of Standard Reference Materials. NASS-4, with certified value of 2.68 ± 0.12 μg/l, was 2.70 μg/l, and for NASS-5 (certified value: 2.6) it was 2.64. Precision was better than ±0.05 ppb. Four aged (>6 months) acidified seawater samples from depths of 700 and 1300 m at the DeepLev site were run through a procedure similar to that of the other samples, and measured by the beta counter for ^{238}U activities.

2.4.2. Particulate organic carbon

POC was determined by a PerkinElmer 2400 CHN Elemental Analyzer. Common organic carbon standards, such as Caffeine, L-glutamic acid, Glycine, and Nicotinamide were used for calibration. Dried samples of particulate matter (on a 25 mm GF/F or as dried powder) were placed in tin or silver cups, fumed by hydrochloric acid (HCl 32%) to remove inorganic carbon, and combusted at 925–1000 °C. The organic carbon was converted to CO_2 and measured by thermal conductivity. The derived POC content per bottle was then translated into fluxes (mg m^{-2} d^{-1}), based on the collection period (mostly, 11 days) and the aperture area (0.5 m^2).

3. Results

3.1. POC

POC fluxes from the DeepLev sediment traps are shown in Figs. 2 and 3, compared with the total mass flux (TMF). Fig. 2 shows 6-month data (Dec 2017 through May 2018) from the three Mclane traps, while in Fig. 3 we show an extended 1.5-yr time series for the deep McLane trap and from the Hydro-Bios traps at 810 and 1490 m (Supplementary Information to Figs. 2 and 3 can be found in (a)).

POC concentrations were typically lower than 10%, with the rest of the material composed predominantly of terrigenous material and

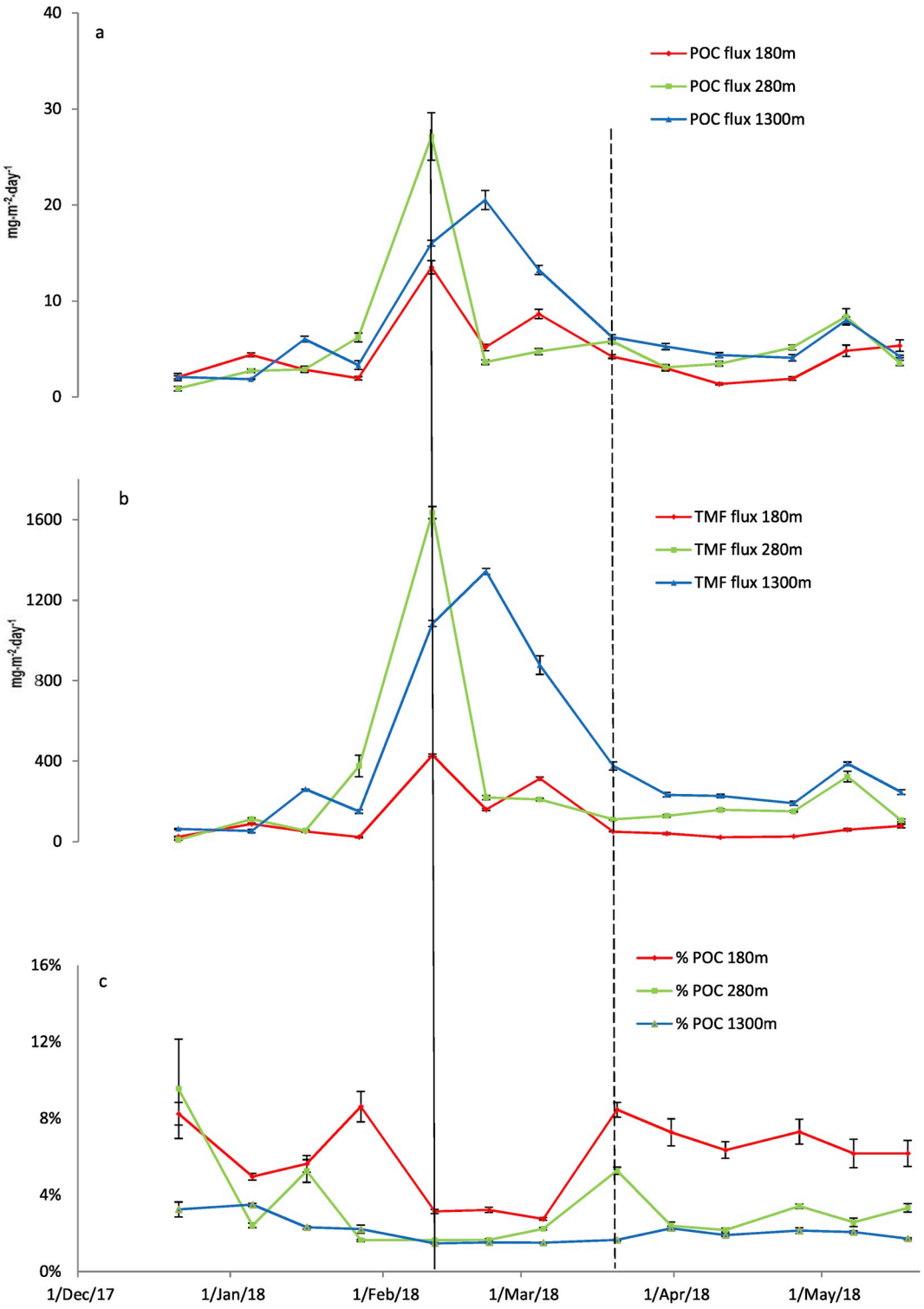

Fig. 2. Time series of (a) particulate organic carbon (POC), (b) total mass flux (TMF) and (c) POC percentage of the TMF, measured by the three automated McLane sediment traps during Dec 2017–May 2018. The vertical black line indicates the strongest rain event of 2018 winter, while the vertical gray line marks the end of the rainy season in this year.

plankton shells (Zlatkin, unpublished results). The most noticeable observation was that POC fluxes where higher in deeper traps (1300 m and 280 m) than at 180 m (averages of 7.3, 6.4 and 4.7 mg m^{-2} day^{-1}, respectively, during Dec 2017 through May 2018, Table 1), which was in correlation with the total mass flux (TMF) (Fig. 2).

Temporal patterns also followed the TMF (Fig. 2). Fluxes were higher during the rainy season, with strong peaks between Jan–March 2018. The highest fluxes were measured in the 280 m (26.9 mg m^{-2} day^{-1}, Feb 2018), while in the 1300 m the flux peak was wider (i.e. sustained for longer period, through the end of March, Fig. 2a), which followed the TMF pattern.

The POC-TMF correlation and the winter peak is supported by the extended time series of the 1300 m trap (Fig. 3a). We also note that fluxes during the 2017–18 winter were significantly higher than in

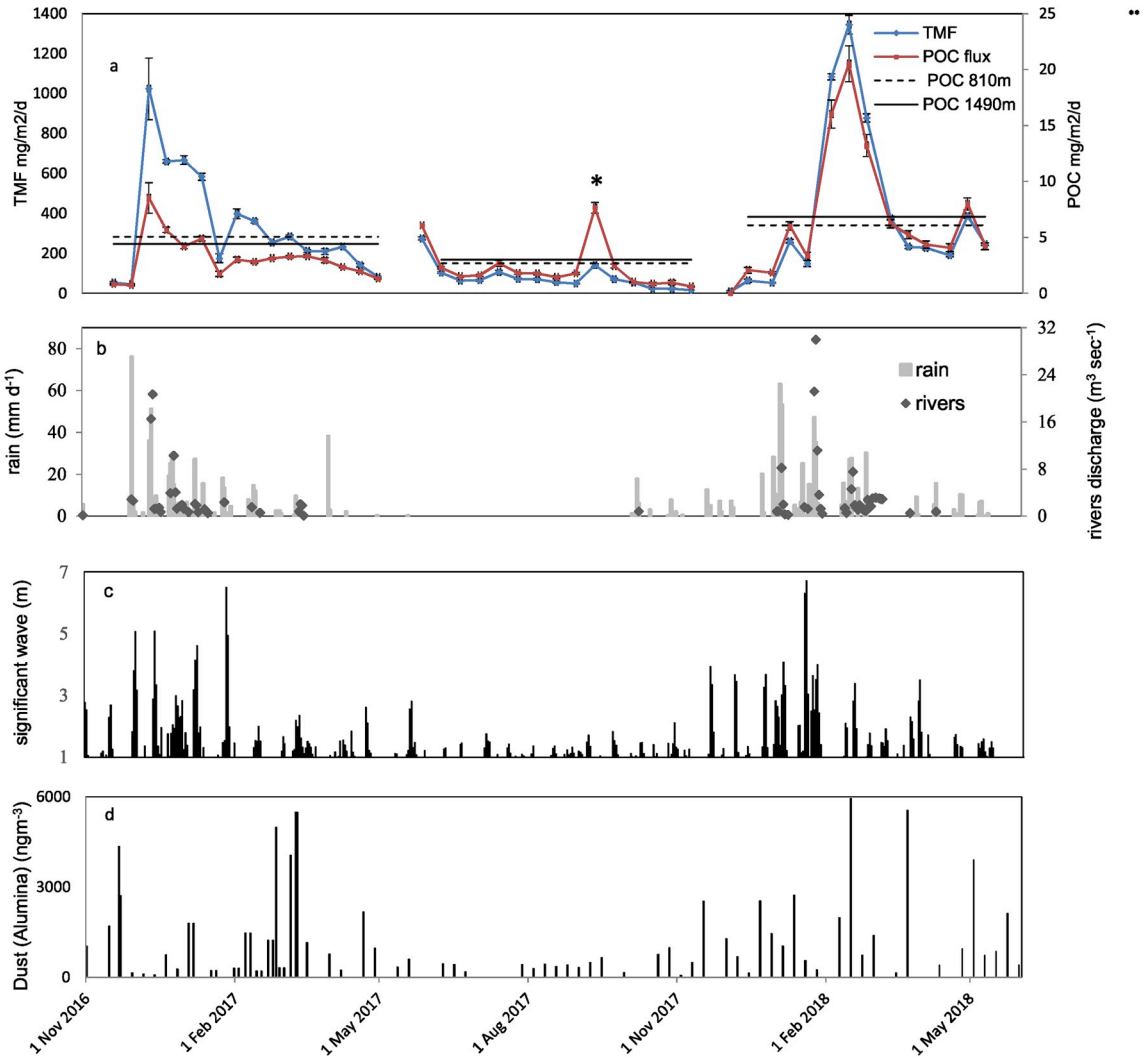

Fig. 3. (a) POC fluxes measured by the McLane sediment trap at 1300 m depth, and by Hydro-Bios cylindrical traps at 810 and 1490 m, compared with total mass flux (TMF); note that the sample marked by (*) was loaded with fish remains; (b) discharge of the Qishon stream (data from the Hydrological Service of Israel) and precipitation in Haifa Port and the Tivon stations (the latter is located ca. 15 km southeast of the first, on the drainage basin of the Qishon stream; data from the Israeli Meteorological Service-IMS); (c) significant wave data (measured 50 km south of Haifa port, data from IOLR)., (d) Aluminum concentrations (ng m^{-3}), as a proxy for dust (measured at IOLR. Haifa).

Table 1
Average and standard deviation of POC flux (mgC m^{-2} d^{-1}) in the traps, arranged by the three deployment periods (numbers in parentheses are the number of samples).

Depth	Nov 16-May 17	June–Nov 17	Dec 17–May 18
180 m	N.A	N.A	4.7 ± 3.5 (13)
280 m	N.A	N.A	6.4 ± 4.7 (13)
810 m*	5.1	2.7	6.1
1,300 m	3.1 ± 1.5 (16)	2.2 ± 1.8 (16)	7.3 ± 5.7 (13)
1,490 m*	4.4	3.1	6.9

*cylindrical (Hydro-Bios) traps.

2016–17 (more than double, Table 1), which is associated with higher precipitation during the 2017-18 season (Fig. 3b). Low and steady fluxes were measured in the 1300 m trap during the spring and summer of 2017 (0.5–2.5 mg m^{-2} day^{-1}), excluding one sample (Sept 11, 2017), where we found abundant fish remains in the collection bottle.

Despite the similar patterns, POC percentages of the total mass were significantly higher in the shallow trap, with averages of 6%, compared with 3.4% and 2% at 280 m and 1300 m, respectively, during Dec 2017 through May 2018 (Fig. 2c). In the 180 m and the 280 m traps, lower POC percentages were observed during and following high flux events (e.g. Feb 2018, Fig. 2c).

POC flux in the cylindrical trap, located at 810 m, was the same as the average for the 1300 m McLane trap (4.4 mg m^{-2} day^{-1}, Fig. 3a and Table 1), although somewhat different when analyzed seasonally (Table 1). In the 1490 m trap (10 m above seafloor), fluxes were slightly higher (Table 1), which is probably due to re-suspension.

3.2. ^{234}Th in water column profiles and on particles

Four ^{234}Th profiles, sampled at DeepLev in May 2017, Dec 2017, Apr 2018 and June 2018, are presented in Fig. 4 and detailed in the Supplementary Information (b). The profiles are shown together with a reference activity of ^{238}U, which is the radioactive parent of ^{234}Th. ^{238}U was measured on samples from three different depths (Table 2), taken during two different cruises, which showed a small range (2.48–2.67 dpm/L). Other samples, taken ca. 100 km south of DeepLev, are also shown and fall within the same concentration range. Uranium concentrations from the literature are usually somewhat higher. Specifically, the updated ^{238}U-salinity relationship, suggested by Pates and Muir (2007) results in ^{238}U = 2.78 dpm/L, which is also shown in Fig. 4.

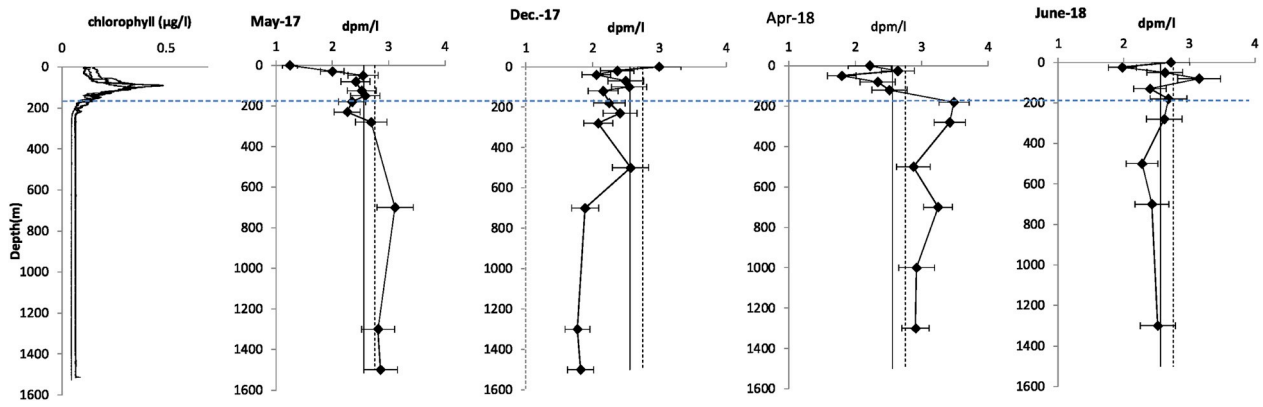

Fig. 4. DeepLev water column profiles of ^{234}Th. The reference ^{238}U profile was determined by measurements from DeepLev (Table 2). U values calculated (Pates and Muir, 2007; Owens et al., 2011) for DeepLev salinities (e.g. Table 2) are also shown. The base of the photic zone is marked by a dashed line at 180 m. Also shown are Chl-a profiles from the same cruises, which exhibit the DCM and the euphotic zone.

Table 2
Uranium concentrations measured along the DeepLev profile and in a nearby station (100 km to the south).

sampling	location	depth	salinity	concentration	activity
		m	psu	µg/L	dpm/L
May 13 2019	DeepLev	50	38.83	3.47	2.53
July 31, 2018	DeepLev	700	38.87	3.66	2.67
May 13 2019	DeepLev	700	38.75	3.40	2.48
July 31, 2018	DeepLev	1300	38.87	3.50	2.55
March 28, 2019	DeepLev	1300	N.A	3.52	2.57
April 10, 2018	Herzliya transect	50	39.24	3.47	2.53
April 10, 2018	Herzliya transect	500	38.83	3.52	2.57
April 10, 2018	Herzliya transect	1000	38.76	3.35	2.45

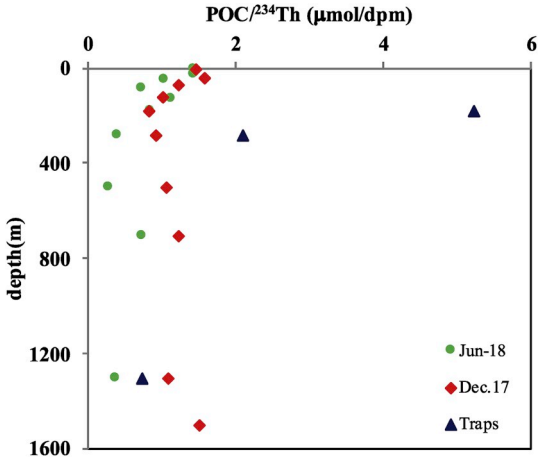

Fig. 5. Profiles of POC/^{234}Th ratios on suspended material, as measured in water column samples (red and green squares; Dec 4, 2017 and June 3, 2018) and on sinking material collected by sediment traps at three depths (May 2018, blue triangles). (For interpretation of the references to colour in this figure legend, the reader is referred to the Web version of this article.)

All four profiles showed minor ^{234}Th deficits (i.e. disequilibrium with ^{238}U) in surface water. However, summing up for the whole euphotic zone, down to 180 m, the profiles of Apr-18 and June-18 seem to exhibit no deficit, and the latter even shows a slight ^{234}Th excess (Fig. 4). This could slightly change in favor of the deficit, if the higher ^{238}U of Pates and Muir (2007) is used (Fig. 4). Nevertheless, the most striking features are the prominent deep water deficit in Dec 2017 and the excess during April 2018 and May 2017, with both prevailing through the whole water column. Unfortunately, we do not have profiles from mid-summer.

Thorium activities were also measured on sinking (traps) and suspended particulate matter (water column sampling). ^{234}Th was significantly lower on particles from the shallow traps (180 and 280 m) compared with the 1300 m trap (1.0–1.1 dpm mg^{-1}, compared with 2.0 dpm mg^{-1}, during May 2018). Accordingly, and due to the lower percentage of POC in the deeper traps, POC/^{234}Th ratios significantly decreased from the 180 m through the 280 and 1300 m traps (5.65, 2.26 and 0.78 µmol dpm^{-1}, respectively, Fig. 5), in agreement with Buesseler et al. (2006). On the other hand, POC/^{234}Th ratios in suspended material along the water column were all <1.6 µmol dpm^{-1} (Dec 2017, June 2018, Fig. 5).

4. Discussion

Marine carbon export is usually associated and being driven by primary production (e.g. Volk and Hoffert, 1985; Ducklow et al., 2001). This implies a strong correlation between C export and PP (Buesseler and Boyd, 2009; Haskell et al. 2013; Frigstad et al., 2015), with higher fluxes during algae blooms (e.g. Rutgers van der Loeff et al. 1997; Foster and Shimmield, 2002; Schmidt et al., 2013). This is true also for continental margins, where research shows that their high PP, considering their respective area (e.g. Eppley and Peterson, 1979), and their high organic matter preservation results in relatively high C-export (e.g. Liu et al., 2000; Chen et al., 2008).

Winter mixing and upwelling of nutrients in the eastern Mediterranean, in particular in the southeastern Levantine Basin, produce higher algal production during winter and early spring, with photic zone chlorophyll concentrations peaking annually from December through February and March (e.g. D'Ortenzio, 2003; Groom et al., 2005; Krom et al., 2010). Our trap data also demonstrate peaks of POC fluxes during this period (Figs. 2 and 3). Yet, our data also reveals that although the mooring is stationed at a deep basin, C export in this area is strongly impacted by terrestrial or shelf processes (see also Karageorgis et al., 2008). This is suggested by several observations. First, we found significantly higher POC fluxes in the deeper traps (1300 and 280 m), compared with fluxes at the base of the photic zone (180 m, Fig. 2). This suggests that POM does not necessarily arrive at depth through vertical sinking, but rather via lateral transport. Second, carbon flux correlated positively with fluxes of total particulate matter, although the POC comprises only a small fraction of the total flux (annually ~5% at 180 m, see below), which gets even lower during flux peaks (3.5% at 180 m, while 2%, in both 280 and the 1300 m traps, Fig. 2). Third, the

coincidence of POC flux peaks with flood events in coastal streams (Spearman correlation coefficient of 0.8), as well as with onshore rain and significant wave records (Fig. 3b-c), suggests that terrestrial discharge, and/or shelf processes, are major drivers of particulate matter and C export in the deep basin of the southeastern Levant. The low POC in traps from mid-March, in particular in the 180 m trap (Fig. 2a), also supports a scenario related to winter events rather than to primary production, which supposedly continues into March–April (Lazzarri et al. 2012). Dust inputs are also higher in winter, but correlation is weaker (Spearman correlation coefficient of 0.2), in particular in the 2016–17 winter (Fig. 3d).

4.1. C export

POC fluxes measured in the trap at the bottom of the photic zone (180 m) ranged between 0.7 and 13.5 mgC m^{-2} d^{-1} during Dec 2017–May 2018 (winter). Using the lowest value (0.7 mgC m^{-2} d^{-1}) as summer flux, we arrive at an approximate annual flux of 0.79 gC m^{-2} yr^{-1}, which is ca. 1% of the typical primary production in this area (Krom et al., 2010). We note that based on the discussion above, specifically the tight correlation with TMF and with fluxes in the deeper traps, we cannot disregard the possibility that some of the carbon at the base of euphotic zone also arrives laterally from the coast/shelf, which implies that PP-related C export could even be lower than 1%. Fluxes measured by Moutin and Raimbault (2002) in June 1996 in four stations at the western Levantine Basin, using free floating cylindrical traps, were significantly higher than those measured in May 2018 at DeepLev (4.5–20.5 mgC m^{-2} d^{-1} at 200 m depth, compared with 2–5 mgC m^{-2} d^{-1}), and percentages of organic carbon were also higher (1.2–12.5%). The differences in measured fluxes could be related to the collection efficiency of the conical traps compared with the free floating traps (Gust et al., 1994), since current speed appears to decrease the efficiency of moored traps by about a factor of three compared with drifting traps. Nevertheless, the lower percentage of organic C in our study, in particular during winter, probably reflects on its terrestrial origin, unlike the western Levantine Basin, which is probably more of marine origin.

POC fluxes at 200 m above seafloor (1300 m depth) ranged between 0.4 and 20.4 mg m^{-2} d^{-1}, with a daily average of 4.2 mg m^{-2} d^{-1} and an annual (June 2017–May 2018) flux of 1.6 gC m^{-2} yr^{-1} (= 0.13 molC m^{-2} yr^{-1}), significantly higher than in the 180 m trap. The daily average documented by the cylindrical traps at 810 and 1490 m were quite similar (4.4 and 5.0 mgC m^{-2} d^{-1}, respectively). While the slightly higher flux at the bottom (1490 m) trap could be the result of resuspension, the very similar average POC fluxes at 1300 and 810 m suggest that the fishing net or the stainless steel mesh that covered the traps opening during most of the reported period did not have a significant impact on its carbon trapping efficiency. The recorded values are very similar to the fluxes found by Stavrakakis et al. (2013) in the deep water of the Ionian Sea (1.12 and 1.63 gC m^{-2} yr^{-1} at 3200 and 4300 m). We note that, unlike for the carbon flux, lower trapping efficiency of the conical traps was observed for the flux of total particulate matter (i.e. lower flux at the 1300 m McLane trap, compared with both the 890 and the 1490 m cylindrical traps, see Katz et al., Table 4, this issue). This is in agreement with the suggested under-capturing of the conical compared with cylindrical traps (e.g. Gust et al., 1994).

The higher flux documented by the 1300 m trap could be related to the lower velocity of currents at depth compared with shallow water (Lazar et al. under revision), which could affect trap efficiency. However, the increase in fluxes is already observed at 280 m (e.g. Fig. 2a), where current velocity is similar to that at 180 m. Accordingly, and as mentioned above, we suggest that the increase in flux with depth is related to the fact that the flux is controlled by lateral input (gravity currents) from land or shelf.

Carbon export could also be tackled with ^{234}Th deficit, which is the ^{234}Th disequilibrium with its radioactive parent ^{238}U (i.e. ^{234}Th/^{238}U activity ratios <1) (e.g. Buesseler et al., 1995; Cochran et al., 1995). Photic zone net ^{234}Th deficits were observed only during May 2017 and Dec 2017 (Fig. 4). Assuming roughly steady state conditions on the ^{234}Th time-scale (mean life time of 35 days) and negligible diffusive and advective fluxes of thorium, ^{234}Th deficits integrated at the base of the euphotic zone (180 m) suggest very similar ^{234}Th fluxes of 1249 (±490) and 1145 (±449) dpm m^{-2} d^{-1}, respectively, during May and Dec 2017 (Table 3 and Fig. 6a). On the other hand, during April and June 2018, practically no flux was observed (Table 3).

Table 3
Calculated fluxes[a] of ^{234}Th and POC[b].

	^{234}Th (180 m)	^{234}Th (1300 m)	POC(180 m)	POC(1300 m)
	dpm m^{-2} d^{-1}	dpm m^{-2} d^{-1}	mmol m^{-2} d^{-1}	mmol m^{-2} d^{-1}
May 2017	1249 (±490)	-9348 (±2980)	1.68 (±0.68)	-7.20 (±2.49)
Dec 2017	1145 (±449)	17,929 (±5512)	1.27 (±0.51)	20.08 (±6.56)
Apr 2018	161 (±74)	-16,602 (±5301)	0.39 (±0.17)	-12.84 (±4.49)
June 2018	-215 (±91)	2916 (±972)	-0.05 (±0.02)	1.43 (±0.55)

[a] 1-D equation (e.g. Coale and Bruland, 1985), assuming steady state and no ^{234}Th diffusion or advection; positive values are for net deficit (^{234}Th) and export (POC), and negative values are for net excess (^{234}Th) and remineralization (POC).

[b] Based on water column POC/^{234}Th, measured during Dec 2017 and June 2018 and averaged for May 2017 and Apr 2018; detailed POC/^{234}Th presented in Fig. 5 and Supplementary Information (b).

Unlike the euphotic zone, DeepLev deep water profiles were mostly (except for June 2018) characterized by ^{234}Th–^{238}U disequilibrium, with that of Dec 2017 showing a clear deficit and those of Apr (2018) and May 2017 portraying excesses (Fig. 4). These translate into relatively large net deep water flux (16,783 dpm m^{-2} d^{-1} in Dec 2017) or remineralization (e.g. 16,763 dpm m^{-2} d^{-1} in Apr, 2018; Table 3). We note that although the clear deep water off-equilibrium patterns, vertical resolution is very low, which is manifested by the errors quoted in Table 3). Therefore, excess and re-mineralization values should be taken with caution. Also note that we did not include the measurements at 1500 m, as to avoid resuspension effects.

While deep water often shows excess ^{234}Th, interpreted as remineralization (e.g. Savoye et al., 2004; Maiti et al., 2010; Planchon et al., 2013), the total water column (including surface water) usually presents a positive flux or a balanced one (i.e. net or zero flux to the seabed). This apparently is not the case in the May 2017 and Apr 2018 DeepLev profiles, where the total water column suggests net remineralization (Table 3 and Fig. 6a). Similarly, the large deficit, therefore net deep water flux, in Dec 2017 is also hard to explain. Intermediate to deep water deficits (i.e. scavenging) were hardly observed in the open ocean (e.g. Baskaran et al., 1996; Benitez-Nelson et al., 2001; Coppola et al., 2005; Owens et al., 2011), and when noted it was usually in margins environments, such as the case of Mediterranean outflow water just off the Gibraltar Straits (Schmidt, 2006), which is due to sediment resuspension and nepheloid layer formation. Altogether, these deep water observations, together with the larger fluxes observed in the deep traps, are better explained by lateral transport, as suggested above, and which will be elaborated below.

In order to calculate POC fluxes, we had to choose between the relatively high POC/^{234}Th ratio measured on trap particles at 180 m and those measured on water column particulate matter (5.65 and 0.83 μmoleC/dpm, end of May-June 2018, Fig. 5). We suspect that the traps did not necessarily capture all sinking particles, especially slowly-sinking small particles (Haskell et al. 2013), an effect which could be amplified if some fish remnants (described in Methods) managed to enter the shallow traps. This, together with the above-suggested lateral transport, could cause the large difference between the POC/^{234}Th

Table 4
Annual, winter and summer TMF and mean weight fraction (%) of POC in the mass flux in automated (AT) and single bottle (SBT) sediment traps from the DeepLev mooring station. In traps placed deeper than 800 m, winter values are the average between the two winter deployments (Nov 2016–Jun 2017 and Dec 2017). Summer values in these traps are from the Jun 2017 to Nov 2017 deployment. Annual values in these deeper traps are calculated as the weighted average between two winters and one summer deployments. In the shallow, automated traps at 180 m and at 280 m, TMF and POC (%) were calculated only for the measured winter deployment.

depth (m)	Trap type	Annual TMF (mg m-2 d-1)	Winter TMF (mg m-2 d-1)	Summer TMF (mg m-2 d-1)	Annual POC %	Winter POC%	Summer POC%
180	AT	na	105	na	na	4.3	na
280	AT	na	274	na	na	2.2	Na
810	SBT	271	445	96	1.5	1.2	2.9
1300	AT	223	379	77	1.6	1.4	2.7
1492	SBT	311	311	142	1.4	1.1	2.1

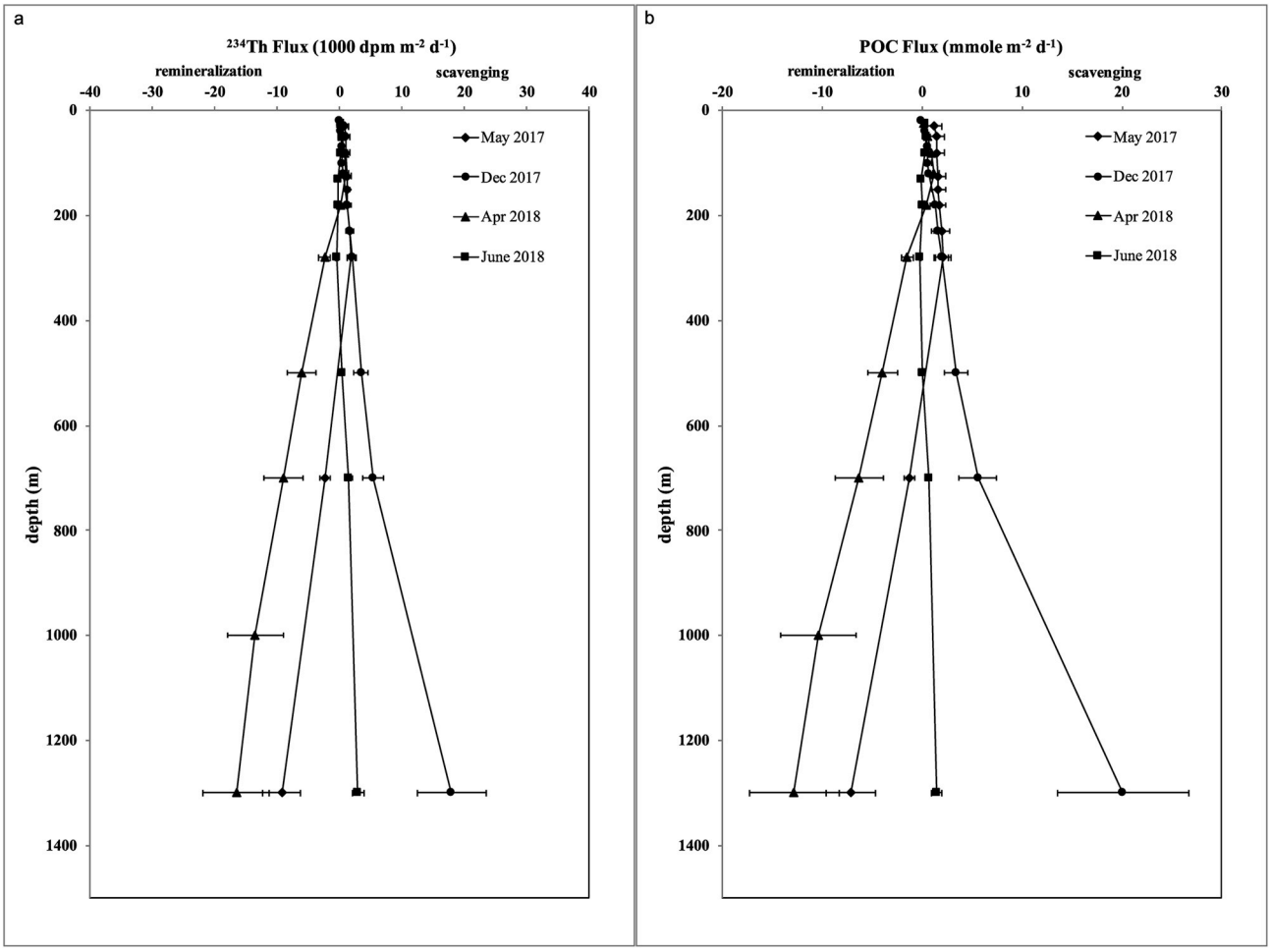

Fig. 6. Calculated integrated water column (a) ^{234}Th fluxes and (b) POC fluxes. Positive is for export, while negative suggests re-mineraliztion.

measured on particles captured and not captured by the traps.

Using, conservatively, the depth-specific POC/^{234}Th measured on water column particles (Fig. 5, Supplementary Information (b)), the calculated POC fluxes at the base of the euphotic zone (180 m) were 0.4–1.7 mmolC m^{-2} d^{-1} during May 2017, Dec 2017 and April 2018 (Table 3), which is similar or slightly lower than export values found in other oligotrophic basins (e.g. Hung et al. 2010; Le Moigne et al. 2013; Owens et al. 2015; Puigcorbé et al., 2017). While in April 2018 there is a good agreement between the thorium-based and the trap-measured POC at 180 m (0.1 and 0.05 mmolC m^{-2} d^{-1}, respectively; compare Table 3 and Fig. 2a), this is not the case for Dec 2017, where the ^{234}Th-based calculation results in a flux of 1.3 mmolC m^{-2} d^{-1}, compared with 0.1–0.2 mmolC m^{-2} d^{-1} in the trap (Fig. 2a). Under-capturing of traps was already suggested by several authors (e.g. Gardner, 1980; Haskell et al. 2013), and the large differences between trap and ^{234}Th assessments were explained by a slow-sinking organic matter, which is documented by the thorium but does not necessarily enter the traps (Haskell et al. 2013). The absence of deficit in June 2018 (even slight excess) suggests that no export occurred during this period (Table 3). Unfortunately, we have no comparable trap data from this time.

Combining the above-shown ^{234}Th fluxes (Fig. 6a) and water column POC/^{234}Th ratios (Fig. 5 and Supplementary Information b), it was only during Dec 2017 that we observed net C export toward the seafloor (Fig. 6a), where most of it did not originate from surface water/photic zone. On the other hand, during the spring-beginning of summer (May 2017, Apr, 2018), there was apparently a net remineralization, which will be further discussed below. Neither export nor remineralization was observed in June 2018.

4.2. The DeepLev deep water enigma

Both the traps and the ^{234}Th signal suggest that the deep water at DeepLev is at least partly decoupled from surface water processes and is fed by lateral transport of shelf or land-derived material. This is implied both by the higher fluxes of POC and TMF recorded in the deeper traps (Fig. 2) and by the large net deep water export or remineralization calculated from the ^{234}Th profiles (Fig. 6). This is somewhat similar to patterns from the northwestern Mediterranean (the Rhône continental margin), where 210 Pb budget and ^{210}Po/^{210}Pb ratios were used to imply on land (riverine) and slope-derived origin for particulate matter (Heussner et al., 1990b; Radakovitch et al., 1999).

Interestingly, while during June 2018 there is an agreement between trap observation and the ^{234}Th-calculated fluxes (hardly any flux), this is not the case with the other profiles. In Dec 2017, the 1300 m trap showed the lowest fluxes recorded at this depth during the 18 months of deployment (<0.05 mmol m^{-2} day^{-1}, Supp. Info. a), while the ^{234}Th implies a large deep water flux. Moreover, the small fluxes documented during May 2017 and Apr 2018 (0.1–0.4 mmol m^{-2} day^{-1}, Supp. Info. a) are not accompanied by ^{234}Th water column fluxes. Instead, in both profiles, there is a negative balance, which apparently implies excess remineralization.

It is suggested that all these observations relate to the predominance of lateral transport by gravity currents in the southeastern Levantine basin. While this kind of transport adds particulate matter to the deep water, which is not related to primary production at surface water, the impact of this transport on the ^{234}Th balance of the deep water is dependent on a variety of parameters, including its POC content. When the gravity current is POC-rich, remineralization predominates, which results in ^{234}Th excess, while when organic matter is low, scavenging outweighs remineralization. It should be noted that in this case, remineralization (and deep ^{234}Th deficits) implies utilization of some of the laterally-transported POC and its transformation into DOC or CO_2, but it by no means implies that there is no export of leftovers to the seabed, which could be reflected in the flux measured in the 1300 m trap during May 2017 and April 2018. Nevertheless, the differences mentioned above between the methods do not allow the calculation of 'remineralization efficiency'. Moreover, some of the particulate matter could be carried laterally farther offshore, therefore it is not reflected as sinking material in the traps.

Based on the ^{234}Th profiles we note that maximum remineralization occurred during spring time (April 2018), at the end of the rainy season, and less or none in the beginning of the dry season (May 2017 and June 2018, respectively, Fig. 6). The deep water deficit observed in December 2017, occurred just at the end of the dry season (Dec 4), before any significant onshore discharge occurred (Fig. 3b). On the other hand, it was preceded by a storm during the end of November 2017, which resulted in significant waves larger than 3 m measured at the inner shelf (2 km offshore, Fig. 2c). It is suggested that while the April 2018 and May 2017 remineralization profiles were based on fine material, which was 'leftover' from onshore discharge, rich with organic matter, the scavenging reflected in the Dec 2017 profile was the result of shelf or upper slope resuspension of relatively organic matter-poor material, which resulted in no or low re-mineralization, with net scavenging of ^{234}Th.

Unfortunately, we do not have profiles from the midst of rainy season (Jan–March), as well as from the middle of the summer, which could shed more light on this deep water enigma.

5. Conclusions

This paper presents the first results of POC fluxes from the deep southeastern Levantine Basin (the DeepLev mooring). The general picture is of coastal or shelf-controlled C export, namely: carbon export occurs due to the introduction of particulate matter of terrestrial or shelf origin by gravity currents to the deep ocean. This results in (1) large seasonal variability, with peaks of export during winter (Dec–Feb) and very low baseline fluxes (mostly, ~0.1 mmolC m^{-2} d^{-1}) during the summer; (2) higher POC fluxes (both peaks and averages) in deep traps (1300 and 280 m) than at the base of euphotic zone (180 m); (3) (transient) large ^{234}Th excess or deficit at depth (e.g. Dec 2017), which imply large remineralization or scavenging at depth.

The suggested lateral transport implies that in the southeastern Levantine Basin export to the seabed, as well as remineralization in twilight zone or deep water, does not have to be balanced by primary production in the euphotic zone. The calculated export to the seabed or remineralization at depth is mainly a balance between the flux arrived at the DeepLev area from shore/shelf and the extent of remineralization it experiences. This balance is not necessarily reflected in the sediment traps due to the mentioned differences between the methods, as well as due to the possible transport of some of the particulate matter farther offshore. This should be further studied by higher resolution measurements of ^{234} Th at depth and by additional profiles farther offshore.

Declaration of competing interest

The authors declare that they have no known competing financial interests or personal relationships that could have appeared to influence the work reported in this paper.

CRediT authorship contribution statement

Ronen Alkalay: Investigation, Data curation, Methodology. **Olga Zlatkin:** Investigation, Data curation. **Timor Katz:** Methodology, Supervision. **Barak Herut:** Conceptualization, Supervision, Funding acquisition. **Ludwik Halicz:** Investigation. **Ilana Berman-Frank:** Conceptualization, Supervision, Funding acquisition. **Yishai Weinstein:** Conceptualization, Investigation, Validation, Writing - review & editing, Funding acquisition.

Acknowledgements

We are grateful to the Council for Higher Education in Israel and the Mediterranean Sea Research Centre of Israel (MERCI), the Wolfson Foundation, the North American Friends of IOLR and Bar-Ilan University (BIU) for funding the construction and maintenance of DeepLev. We owe gratitude to a lot of people, who contributed to the success of DeepLev deployment. This includes the IOLR departments of electronic, sea operations and marine physics and the engineers of the machine shop at BIU. Special thanks to the captain and crew of R/V Bat Galim, who did a great job in the deployment and recovery of the mooring and attached devices. Special thanks to K. Weiss and Y. Zakon for the MC-ICPMS analyses of ^{230}Th. Lastly, we want to thank the anonymous reviewers for their very helpful comments and to Annie Sacio for proof-reading the manuscript. This project was supported by the Israeli Ministries of Energy and Environmental Protection under tdhe framework of the National Monitoring Program for Israeli Mediterranean Waters and by the Israel Science Foundation grant ISF 25/2014.

Appendix A. Supplementary data

Supplementary data to this article can be found online at https://doi.org/10.1016/j.dsr2.2019.104713.

References

Armstrong, R.A., Lee, C., Hedges, J.I., Honjo, S., Wakeham, S.G., 2002. A new, mechanistic model for organic carbon fluxes in the ocean based on the quantitative association of POC with ballast minerals. Deep-Sea Res. Part II Top. Stud. Oceanogr. 49 (1–3), 219–236.

Armstrong, R.A., Peterson, M.L., Lee, C., Wakeham, S.G., 2009. Settling velocity spectra and the ballast ratio hypothesis. Deep-Sea Res. Part II Top. Stud. Oceanogr. 56 (18), 1470–1478.

Azov, Y., 1986. Seasonal patterns of phytoplankton productivity and abundance in nearshore oligotrophic waters of the Levant Basin (Mediterranean). J. Plankton Res. 8 (1), 41–53.

Baskaran, M., Santschi, P.H., Laodong, G., Bianchi, T.S., Lambert, C., 1996. 234Th:238U disequilibria in the Gulf of Mexico: the importance of organic matter and particle concentration. Cont. Shelf Res. 16 (3), 353–380.

Benitez-Nelson, C., Buesseler, K.O., Karl, D.M., Andrews, J., 2001. A time-series study of particulate matter export in the North Pacific Subtropical Gyre based on 234 Th : 238 U disequilibrium. Deep. Res. I 48, 2595–2611.

Berman, T., Townsend, D.W., EI-Sayed, S.Z., Trees, C.C., Azov, Y., 1984. Optical transparency, chlorophyll and primary productivity in the Eastern Mediterranean near the Israeli coast. Oceanol. Acta 7 (3), 367–372.

Berman, T., Walline, P.D., Schneller, A., Rothenberg, J., Townsend, D.W., 1985. Secchi disk depth record: a claim for the eastern Mediterranean. Limnol. Oceanogr. 30 (2), 447–448.

Boyd, P.W., Trull, T.W., 2007. Understanding the export of biogenic particles in oceanic waters: is there consensus? Prog. Oceanogr. 72 (4), 276–312.

Buesseler, K.E.N., Michael, P., Livingston, H.D., Cochrant, K., 1992. Carbon and Nitrogen Export during the JGOFS North Atlantic Bloom Experiment Estimated from 234Th : 23aU Disequilibria 39.

Buesseler, K.O., Andrews, J.A., Hartman, M.C., Belastock, R., Chai, F., 1995. Regional estimates of the export flux of particulate organic-carbon derived from Th-234 during the JGOFS EqPac program. Deep Sea Res. Part II 42 (2–3), 777–804.

Buesseler, Ken O., Benitez-Nelson, C., Rutgers van der Loeff, M., Andrews, J., Ball, L., Crossin, G., Charette, M.A., 2001. An intercomparison of small- and large-volume techniques for thorium-234 in seawater. Mar. Chem. 74, 15–28.

Buesseler, K.O., Benitez-Nelson, C.R., Moran, S.B., Burd, A., Charette, M.A., Cochran, J. K., Coppola, L., Fisher, N.S., Fowler, S.W., Gardner, W.D., Guo, L.D., Gustafsson, O., Lamborg, C., Masque, P., Miquel, J.C., Passow, U., Santschi, P.H., Savoye, N., Stewart, G., Trull, T., 2006. An assessment of particulate organic carbon to thorium-234 ratios in the ocean and their impact on the application of ^{234}Th as a POC flux proxy. Mar. Chem. 100, 213–233.

Buesseler, K.O., Antia, A.N., Chen, M., Fowler, S.W., Gardner, W.D., Gustafsson, O., Harada, K., Michaels, A.F., Rutgers van der Loeff, M., Sarin, M., Steinberg, D.K., Trull, T., 2007. An assessment of the use of sediment traps for estimating upper ocean particle fluxes. J. Mar. Res. 65 (3), 345–416.

Buesseler, K.O., Boyd, P.W., 2009. Shedding light on processes that control particle export and flux attenuation in the twilight zone of the open ocean. Limnol. Oceanogr. 54 (4), 1210–1232.

Cai, P., Dai, M., Lv, D., Chen, W., 2006. An improvement in the small-volume technique for determining thorium-234 in seawater. Mar. Chem. 100, 282–288.

Carlson, C.A., Ducklow, H.W., Michaels, A.F., 1994. Annual flux of dissolved organic carbon from the euphotic zone in the northwestern Sargasso Sea. Nature 371, 405–408.

Chen, W., Cai, P., Dai, M., Wei, J., 2008. ^{234}Th/^{238}U disequilibrium and particulate organic carbon export in the northern south China sea. J. Oceanogr. 64, 417–428.

Coale, K.H., Bruland, K.W., 1985. 234Th:238U disequilibria within the California Current. Limnol. Oceanogr. 30, 22–33.

Cochran, J.K., Barnes, C., Achman, D., Hirschberg, D.J., 1995. Thorium-234/uranium-238 disequilibrium as an indicator of scavenging rates and particulate organic-carbon fluxes in the Northeast Water Polynya, Greenland. J. Geophys. Res. Oceans 100 (C3), 4399–4410.

Coppola, L., Roy-Barman, M., Mulsow, S., Povinec, P., Jeandel, C., 2005. Low particulate organic carbon export in the frontal zone of the Southern Ocean (Indian sector) revealed by 234Th. Deep Sea Res. I 52 (1), 51–68.

D'Ortenzio, F., 2003. Did biological activity in the Ionian Sea change after the Eastern Mediterranean Transient? Results from the analysis of remote sensing observations. J. Geophys. Res. 108 (C9), 8113. https://doi.org/10.1029/2002JC001556.

Danovaro, R., Dinet, A., Duineveld, G., Tselepides, A., 1999. Benthic response to particulate fluxes in different trophic environments: a comparison between the Gulf of Lions-Catalan Sea (western-Mediterranean) and the Cretan Sea (eastern-Mediterranean). Prog. Oceanogr. 44, 287–312.

Ducklow, H.W., Steinberg, D.K., Buesseler, K.O., 2001. Upper ocean carbon export and the biological pump. Oceanography 14 (4), 50–58.

Eppley, R.W., Peterson, B.J., 1979. Particulate organic matter flux and planktonic new production in the deep ocean. Nature 282 (5740), 677–680.

Falkowski, P.G., 1998. Biogeochemical controls and feedbacks on ocean primary production. Science 281 (5374), 200–206. https://doi.org/10.1126/science.281.5374.200.

Foster, J.M., Shimmield, G.B., 2002. ^{234}Th as a tracer of particle flux and POC export in the northern North Sea during a coccolithophore bloom. Deep Sea Res. II 49 (15), 2965–2977.

Frigstad, H., Henson, S.A., Hartman, S.E., Omar, A.M., Jeansson, E., Cole, H., Pebody, C., Lampitt, R.S., 2015. Links between surface productivity and deep ocean particle flux at the Porcupine Abyssal Plain sustained observatory. Biogeosciences 12 (19), 5885–5897.

Gardner, W.D., 1980. Field assessment of sediment traps. J. Mar. Res. 38 (1), 41–52.

Gogou, A., Sanchez-Vidal, A., Durrieu de Madron, X., Stavrakakis, S., Calafat, A.M., Stabholz, M., Psarra, S., Canals, M., Heussner, S., Stavrakaki, I., Papathanassiou, E., 2014. Reprint of: carbon flux to the deep in three open sites of the Southern European Seas (SES). J. Mar. Syst. 135, 170–179.

Groom, S., Herut, B., Brenner, S., Zodiatis, G., Psarra, S., Kress, N., Krom, M.D., Law, C.S., Drakopoulos, P., 2005. Satellite-derived spatial and temporal biological variability in the Cyprus Eddy. Deep Sea Res. II 52 (22–23), 2990–3010.

Gust, G., Michaels, A.F., Johnson, R., Deuser, W.G., Bowles, W., 1994. Mooring line motions and sediment trap hydromechanics: in situ intercomparison of three common deployment designs. Deep Sea Res. I 41 (5–6), 831–857.

Guyennon, A., Baklouti, M., Diaz, F., Palmieri, J., Beuvier, J., Lebaupin-Brossier, C., Arsouze, T., Beranger, K., Dutay, J.C., Moutin, T., 2015. New insights into the organic carbon export in the Mediterranean Sea from 3-D modeling. Biogeosciences 12 (23), 7025–7046.

Hansell, D.A., Carlson, C.A., Repeta, D.J., Schlitzer, R., 2009. Dissolved organic matter in the ocean : a controversy stimulates new insights. Oceanography 22 (4), 202–211.

Haskell, W.Z., Berelson, W.M., Hammond, D.E., Capone, D.G., 2013. Particle sinking dynamics and POC fluxes in the Eastern Tropical South Pacific based on ^{234}Th budgets and sediment trap deployments. Deep Sea Res. I 81, 1–13. https://doi.org/10.1016/j.dsr.2013.07.001.

Henson, S.A., Sanders, R., Madsen, E., 2012. Global patterns in efficiency of particulate organic carbon export and transfer to the deep ocean. Glob. Biogeochem. Cycles 26 (1), 1–14.

Herut, B., Krom, M.D., Pan, G., Mortimer, R., 1999. Atmospheric input of nitrogen and phosphorus to the SE Mediterranean: sources, fluxes and possible impact. Limnol. Oceanogr. 44, 1683–1692.

Herut, B., Collier, R., Krom, M.D., 2002. The role of dust in supplying N and P to the SE Mediterranean. Limnol. Oceanogr. 47, 870–878.

Heussner, S., Ratti, C., Carbonne, J., 1990. The PPS 3 time-series sediment trap and the trap sample processing techniques used during the ECOMARGE experiment. Cont. Shelf Res. 10, 943–958.

Heussner, S., Cherry, R.D., Heyraud, M., 1990. ^{210}Po, ^{210}Pb in sediment trap particles on the Mediterranean continental margin. Cont. Shelf Res. 10, 989–1004.

Honjo, S., Doherty, K.W., 1988. Large aperture time-series sediment traps; design objectives, construction and application. Deep Sea Res. Part A, Oceanogr. Res. Pap. 35, 133–149.

Honjo, S., 1996. Fluxes of particles to the Interior of the open oceans. In: Ittekkot, V. (Ed.), Particle Flux in the Ocean. John Wiley and Sons Ltd, New York, pp. 91–154.

Hung, C.C., Gong, G.C., 2010. POC/234Th ratios in particles collected in sediment traps in the northern South China Sea. Estuar. Coast. Shelf Sci. 88, 303–310.

Karageorgis, A.P., Gardner, W.D., Georgopoulos, D., Mishonov, A.V., Krasakopoulou, E., Anagnostou, C., 2008. Particle dynamics in the Eastern Mediterranean Sea: a synthesis based on light transmission, PMC, and POC archives (1991-2001). Deep Sea Res. I 55 (2), 177–202.

Katz, T., Weinstein, Y., Alkalay, R., Biton, E., Toledo, Y., Lazar, A., Zlatkin, O., Soffer, R., Rahav, E., Sisma-Ventura, G., Bar, T., Ozer, T., Gildor, H., Almogi-Labin, A., Kanari, M., Berman-Frank, I., Herut, B., 2019. The first deep-sea mooring station in the eastern Levantine basin (DeepLev), outline and insights into regional sedimentological processes. Deep Sea Res. II (submitted, this issue).

Kessouri, F., Ulses, C., Estournel, C., Marsaleix, P., D'Ortenzio, F., Severin, T., Taillandier, V., Conan, P., 2018. Vertical mixing effects on phytoplankton dynamics and organic carbon export in the western Mediterranean Sea. J. Geophys. Res. Ocean 123, 1647–1669.

Klaas, C., Archer, D.E., 2002. Association of sinking organic matter with various types of mineral ballast in the deep sea: implications for the rain ratio. Glob. Biogeochem. Cycles 16 (4), 63-1–63-14.

Kress, N., Gertman, I., Herut, B., 2013. Temporal evolution of physical and chemical characteristics of the water column in the Easternmost Levantine basin (Eastern Mediterranean Sea) from 2002 to 2010. J. Mar. Syst. 135, 6–13.

Krom, M.D., Kress, N., Brenner, S., Gordon, L.I., 1991. Phosphorus limitation of primary productivity in the eastern Mediterranean Sea. Limnol. Oceanogr. 36 (3), 424–432.

Krom, M.D., Herut, B., Mantoura, R.F.C., 2004. Nutrient budget for the eastern mediterranean: implications for phosphorus limitation. Limnol. Oceanogr. 49, 1582–1592.

Krom, M.D., Emeis, K.C., Van Cappellen, P., 2010. Why is the Eastern Mediterranean phosphorus limited? Prog. Oceanogr. 85 (3–4), 236–244. https://doi.org/10.1016/j.pocean.2010.03.003.

Lamborg, C.H., Buesseler, K.O., Valdes, J., Bertrand, C.H., Bidigare, R., Manganini, S., Pike, S., Steinberg, D., Trull, T., Wilson, S., 2008. The flux of bio- and lithogenic material associated with sinking particles in the mesopelagic "twilight zone" of the northwest and North Central Pacific Ocean. Deep. Res. Part II Top. Stud. Oceanogr. 55, 1540–1563.

Lazzari, P., Solidoro, C., Ibello, V., Salon, S., Teruzzi, A., Béranger, K., Colella, S., Crise, A., 2012. Seasonal and inter-annual variability of plankton chlorophyll and primary production in the Mediterranean Sea: a modelling approach. Biogeosciences 9 (1), 217–233.

Lazzari, P., Solidoro, C., Salon, S., Bolzon, G., 2016. Spatial variability of phosphate and nitrate in the Mediterranean Sea : a modeling approach. Deep. Res. Part I 108, 39–52.

Le Moigne, F.A.C., Gallinari, M., Laurenceau, E., De La Rocha, C.L., 2013. Enhanced rates of particulate organic matter remineralization by microzooplankton are diminished by added ballast minerals. Biogeosciences 10, 5755–5765.

Liu, K.-K., Atkinson, L., Chen, C.T.A., Gao, S., Hall, J., Macdonald, R.W., McManus, L.T., Quinones, R., 2000. Exploring continental margin carbon fluxes on a global scale. Eos 81 (52), 641–645.

Maiti, K., Benitez-Nelson, C.R., Buesseler, K.O., 2010. Insights into particle formation and remineralization using the short-lived radionuclide, Thoruim-234. Geophys. Res. Lett. 37 (15), 2–7.

Martin, J.H., Knauer, G.A., Karl, D.M., Broenkow, W.W., 1987. VERTEX: carbon cycling in the northeast Pacific. Deep Sea Res. I 34 (2), 267–285.

Moutin, T., Raimbault, P., 2002. Primary production, carbon export and nutrients availability in western and eastern Mediterranean Sea in early summer 1996 (MINOS cruise). J. Mar. Syst. 33–34, 273–288.

Owens, S.A., Buesseler, K.O., Sims, K.W.W., 2011. Re-evaluating the 238 U-salinity relationship in seawater : implications for the U – 234 Th disequilibrium method. Mar. Chem. 127, 31–39.

Owens, S.A., Pike, S., Buesseler, K.O., 2015. Thorium-234 as a tracer of particle dynamics and upper ocean export in the Atlantic Ocean. Deep. Res. Part II Top. Stud. Oceanogr. 116, 42–59.

Ozer, T., Gertman, I., Kress, N., Silverman, J., Herut, B., 2015. Interannual thermohaline (1979-2014) and nutrient (2002-2014) dynamics in the Levantine surface and intermediate water masses, SE Mediterranean Sea. Glob. Planet. Chang. https://doi.org/10.1016/j.gloplacha.2016.04.001.

Pates, J.M., Muir, G.K.P., 2007. U–salinity relationships in the Mediterranean: implications for 234Th:238U particle flux studies. Mar. Chem. 106 (3–4), 530–545.

Pike, S., Buesseler, K.O., Andrews, J., Savoye, N., 2005. Quantification of 234Th recovery in small volume seawater samples by inductively coupled plasma mass spectrometry. J. Radioanal. Nucl. Chem. 263, 355–360.

Planchon, F., Cavagna, A.-J., Cardinal, D., André, L., Dehairs, F., 2013. Late summer particulate organic carbon export and twilight zone remineralisation in the Atlantic sector of the Southern Ocean. Biogeosciences 10 (2), 803–820.

Psarra, S., Tselepides, A., Ignatiades, L., 2000. Primary productivity in the oligotrophic Cretan Sea (NE Mediterranean): seasonal and interannual variability. Prog. Oceanogr. 46 (2–4), 187–204.

Puigcorbé, V., Masqué, P., Roca-Martí, M., et al., 2017. Latitudinal distributions of particulate carbon export across the North western atlantic ocean. Deep-Sea Res. Part I 129, 116–130.

Radakovitch, O., Cherry, R.D., Heussner, S., 1999. 210Pb and 210Po: tracers of particle transfer on the Rhône continental margin (NW Mediterranean). Deep Sea Res. Oceanogr. Res. Pap. 46 (9), 1539–1563.

Ramondenc, S., Goutx, M., Lombard, F., Santinelli, C., Stemmann, L., Gorsky, G., Guidi, L., 2016. An initial carbon export assessment in the Mediterranean Sea based on crossmark drifting sediment traps and the Underwater Vision Profiler data sets. Deep Sea Res. I 117, 107–119.

Roy-Barman, M., Coppola, L., Souhaut, M., 2002. Thorium isotopes in the western Mediterranean Sea: an insight into the marine particle dynamics. Earth Planet. Sci. Lett. 196 (3–4), 161–174.

Rutgers Van Der Loeff, M.M., Friedrich, J., Bathmann, U.V., 1997. Carbon export during the spring bloom at the antarctic polar front, determined with the natural tracer 234Th. Deep Sea Res. Part II 44 (1–2), 457–478.

Rutgers van der Loeff, M.M., Sarin, M.M., Baskaran, M., Benitez-Nelson, C., Buesseler, K. O., Charette, M., Dai, M., Gustafsson, Ö., Masque, P., Morris, P.J., Orlandini, K., Rodriguez-Baena, A., Savoye, N., Schmidt, S., Turnewitsch, R., Vöge1, I., Waples, J. T., 2006. A review of present techniques and methodological advances in analyzing ^{234}Th in aquatic systems. Mar. Chem. 100, 190–212. http://doi:10.1016/j.marchem.2005.10.012.

Savoye, N., Buesseler, K.O., Cardinal, D., Dehairs, F., 2004. ^{234}Th deficit and excess in the Southern Ocean during spring 2001: particle export and remineralization. Geophys. Res. Lett. 31, 4–7.

Schmidt, S., 2006. Impact of the mediterranean outflow water on the particle dynamics in intermediate waters of the northeast atlantic as revealed by Th- 234 and Th-228. Mar. Chem. 100, 289–298.

Schmidt, S., Harlay, J., Borges, A.V., Groom, S., Delille, B., Roevros, N., Christodoulou, S., Chou, L., 2013. Particle export during a bloom of Emiliania huxleyi in the North-West European continental margin. J. Mar. Syst. 109–110. https://doi.org/10.1016/j.jmarsys.2011.12.005.

Siegel, D.A., 2014. Global assessment of ocean carbon export by combining satellite observations and food-web models. Glob. Biogeochem. Cycles 28 (2), 181–196.

Speicher, E.A., Moran, S.B., Burd, A.B., Delfanti, R., Kaberi, H., Kelly, R.P., Papucci, C., Smith, J.N., Stavrakakis, S., Torricelli, L., Zervakis, V., 2006. Particulate organic carbon export fluxes and size-fractionated POC/234Th ratios in the Ligurian, Tyrrhenian and Aegean Seas. Deep Sea Res. I 53 (11), 1810–1830.

Stavrakakis, S., Gogou, A., Krasakopoulou, E., Karageorgis, A.P., Kontoyiannis, H., Rousakis, G., Velaoras, D., Perivoliotis, L., Kambouri, G., Stavrakaki, I., Lykousis, V., 2013. Downward fluxes of sinking particulate matter in the deep Ionian Sea (NESTOR site), eastern Mediterranean: seasonal and interannual variability. Biogeosciences 10, 7235–7254.

Stern, N., Alkalay, R., Lazar, A., Katz, T., Weinstein, Y., Berman- Frank, I., Herut, B., 2019. Unexpected massive enmeshments of the sharpchin barracudina paralepis coregonoides Risso, 1820 in mesopelagic sediment traps in the Levantine Basin, SE Mediterranean Sea. Mediterr. Mar. Sci. https://doi.org/10.12681/mms.20747. https://doi.org/10.12681/mms.20747.

Tanaka, T., Thingstad, T.F., Gasol, J.M., Cardeluz, C., Jezbera, J., Sala, M.M., Imek, K., Unrein, F., 2009. Determining the availability of phosphate and glucose for bacteria in P-limited mesocosms of NW Mediterranean surface waters. Aquat. Microb. Ecol. 56 (1), 81–91. http://www.int-res.com/abstracts/ame/v56/n1/p81-91/.

Tanaka, T., Thingstad, T.F., Christaki, U., Colombet, J., Cornet-Barthaux, V., Courties, C., Grattepanche, J.D., Lagaria, A., Nedoma, J., Oriol, L., Psarra, S., Pujo-Pay, M., Van Wambeke, F., 2011. Lack of P-limitation of phytoplankton and heterotrophic prokaryotes in surface waters of three anticyclonic eddies in the stratified Mediterranean Sea. Biogeosciences 8 (2), 525–538.

Thingstad, T.F., Krom, M.D., Mantoura, R.F.C., 2005. Nature of phosphorus limitation in the ultraoligotrophic eastern mediterranean. Science 309 (5737), 1068–1072. https://doi.org/10.1126/science.1112632.

Thomas, D.N., Lara, R.J., Eicken, H., Kattner, G., Skoog, A., 1995. Dissolved organic matter in Arctic multi-year sea ice during winter: major components and relationship to ice characteristics. Polar Biol. 15 (7), 477–483.

Van Wambeke, F., Christaki, U., Giannakourou, A., Moutin, T., Souvemerzoglou, K., 2002. Longitudinal and vertical trends of bacterial limitation by phosphorus and carbon in the Mediterranean Sea. Microb. Ecol. 43 (1), 119–133.

Volk, T., Hoffert, M.I., 1985. Ocean carbon pumps: analysis of relative strength and efficiencies in ocean-driven atmospheric CO_2 changes. Geophys. Monogr. Ser. 32, 99–110.

Wakeham, S.G., Lee, C., Peterson, M.L., Liu, Z., Szlosek, J., Putnam, I.F., Xue, J., 2009. Organic biomarkers in the twilight zone-Time series and settling velocity sediment traps during MedFlux. Deep. Res. Part II Top. Stud. Oceanogr.

Waples, J.T., Benitez-nelson, C., Savoye, N., 2006. An Introduction to the Application and Future Use of in Aquatic Systems, 100, pp. 166–189.

Yu, E.-F., Francois, R., Bacon, M., Honjo, S., Fleer, A., Manganini, S., Rutgers van der Loeff, M., Ittekot, V., 2001. Trapping efficiency of bottom-tethered sediment traps estimated from the intercepted fluxes of and. Deep-Sea Res. Part I Oceanogr. Res. Pap. 48, 865–889.

Zohary, T., Robarts, R.D., 1998. P limitation in the eastern of microbial Mediterranean Experimental study. Limnol. Oceanogr. 43 (3), 387–395.